Contribution from the Department of Chemistry, University of Western Ontario, London, Ontario, Canada N6A 5B7, and Chemistry Department, University of Glasgow, Glasgow G12 8QQ, Scotland, U.K.

A 46-Electron Trinuclear Cluster of Platinum with Strong Pt–Pt Bonds: Synthesis and Structure of $[Pt_3(\mu\text{-}CO)(\mu\text{-}Me_2PCH_2PMe_2)_4][BPh_4]_2$

Samson S. M. Ling,[1a] Nasim Hadj-Bagheri,[1a] Ljubica Manojlović-Muir,*[1b] Kenneth W. Muir,[1b] and Richard J. Puddephatt*[1a]

Received May 13, 1986

The trinuclear cluster cation $[Pt_3(\mu\text{-}CO)(\mu\text{-}dmpm)_4]^{2+}$, dmpm = $Me_2PCH_2PMe_2$, is formed by reaction of $[Pt_2(\mu\text{-}dmpm)_3(PPh_3)]$ with CO in aqueous methanol. It has been characterized spectroscopically as the $[PF_6]^-$ salt and crystallographically as the $[BPh_4]^-$ salt. Crystals of $[Pt_3(\mu\text{-}CO)(\mu\text{-}dmpm)_4][BPh_4]_2\cdot(CH_3)_2CO$ are monoclinic, space group $P2_1/n$, with a = 23.040 (2) Å, b = 14.367 (1) Å, c = 23.823 (1) Å, β = 103.95 (1)°, and Z = 4; R = 0.032 for 8106 independent structure amplitudes. The complex cation contains a Pt_3 triangle in which all three edges are bridged by dmpm ligands to form a latitudinal Pt_3P_6 skeleton. The fourth dmpm ligand and CO bridge the Pt(1)–Pt(3) bond in longitudinal μ fashion. The cation appears to be the first 46e triangulo trinuclear cluster of platinum to be characterized. Remarkably, in view of previous theoretical predictions, the Pt–Pt bond lengths of 2.620 (1)–2.648 (1) Å are very similar to those in the 42e cluster $[Pt_3(\mu_3\text{-}CO)(\mu\text{-}dppm)_3]^{2+}$, dppm = $Ph_2PCH_2PPh_2$. The cation reacts slowly with ^{13}CO and MeNC to give $[Pt_3(\mu\text{-}^{13}CO)(\mu\text{-}dmpm)_4]^{2+}$ and $[Pt_3(\mu\text{-}CNMe)(\mu\text{-}dmpm)_4]^{2+}$, respectively, but fails to react with many other unsaturated reagents (e.g. SO_2, CS_2, PhCCPh). It is concluded that the 46e configuration of the trinuclear cation is favorable and that ligand dissociation to give the more common 44e or 42e clusters does not occur readily.

Introduction

The most common electron count for trinuclear clusters of platinum and palladium is 42e. Some typical examples with μ ligands include $[Pt_3(\mu\text{-}CO)_3L_3]$ (L = $P(cy)_3$ (cy = C_6H_{11})), $[Pt_3(\mu\text{-}SO_2)_3L_3]$ (L = PPh_3), and $[Pt_3(\mu\text{-}H)(\mu\text{-}PPh_2)_2L_3]^+$ (L = PPh_3).[2,3] Another example, but with a μ_3 ligand, is $[Pt_3(\mu_3\text{-}CO)(\mu\text{-}dppm)_3]^{2+}$ (dppm = $Ph_2PCH_2PPh_2$).[4] In these compounds each platinum center has a 16e configuration and forms two Pt–Pt bonds. Although the 18e configuration is usual for platinum(IV) and is known in many other platinum complexes, especially of platinum(0), addition of further ligands to the 42e clusters leads to lengthening, and presumably weakening, of the metal–metal bonds. The effect is modest in zero-oxidation-state complexes, but the Pt–Pt bonds in the 44e complexes $[Pt_3(\mu\text{-}CO)_3L_4]$ (L = $P(cy)_3$) and in $[Pt_3(\mu\text{-}SO_2)_3L_2L'_2]$ (L = $P(cy)_3$ and L'_2 = $Ph_2P(CH_2)_3PPh_2$) are longer than in the 42e counterparts.[2,3,5–7] For example, the Pt–Pt distances in $[Pt_3(CO)_3L_3]$ and $[Pt_3(CO)_3L_4]$ fall in the ranges 2.653–2.656 and 2.675–2.736 Å, respectively, when L = $P(cy)_3$.[1,5] Indeed, reactions of these clusters with smaller phosphine ligands lead to breakdown to mononuclear fragments.[8,9] In higher oxidation state clusters the effect is more dramatic. In one isomeric form of the 44e cluster $[Pt_3Ph(\mu\text{-}PPh_2)_3(PPh_3)_2]$, one Pt–Pt distance of 3.63 Å is clearly nonbonding,[10] though in related compounds a general increase in all metal–metal distances is observed.[10,11] Furthermore, in the 46e cluster $[Pd_3(\mu_3\text{-}S)(CN)(\mu\text{-}dppm)_3]^+$ there is only one Pd–Pd bond[12] and in the 48e cluster $[Pt_3(\mu_3\text{-}S)_2(PMe_2Ph)_6]^{2+}$ there appears to be no metal–metal bonding.[13] This weakening of metal–metal bonding in trinuclear clusters of platinum and palladium for electron counts over 42e has been rationalized by theoretical treatments.[14,15] It is thought that the extra electrons occupy orbitals that have cluster antibonding character.

In this paper the rare 46e trinuclear cluster cation $[Pt_3(\mu\text{-}CO)(\mu\text{-}dmpm)_4]^{2+}$ (**1**; dmpm = $Me_2PCH_2PMe_2$) is reported. Remarkably, in view of all the precedents cited above, the Pt–Pt bond distances in this compound are not significantly different from those in the related 42e cluster $[Pt_3(\mu_3\text{-}CO)(\mu\text{-}dppm)_3]^{2+}$ and this, together with the low chemical reactivity, suggests that the 46e configuration for **1** is not unfavorable and does not lead to weakening of the Pt–Pt bonds or to labilization of the carbonyl or dmpm ligands.

Results

Synthesis of the Cluster Cation. Reaction of $[Pt_2(\mu\text{-}dmpm)_3(PPh_3)]$ with carbon monoxide in aqueous methanol at 100 °C gave the cluster cation $[Pt_3(\mu\text{-}CO)(\mu\text{-}dmpm)_4]^{2+}$ (**1**), which could be precipitated as either the $[PF_6]^-$ or $[BPh_4]^-$ salt, **1a** or **1b**, respectively, in good yield. The simplest equation for this transformation is given by eq 1.

$$3[Pt_2(\mu\text{-}dmpm)_3(PPh_3)] + 2CO + 4H_2O \rightarrow 2[Pt_3(\mu\text{-}CO)(\mu\text{-}dmpm)_4]^{2+} + 3PPh_3 + dmpm + 4OH^- + 2H_2 \quad (1)$$

All of these species were identified in the crude reaction product. However, this equation is an oversimplification since CO_2 is also formed, either by a stoichiometric reaction or by some catalysis of the water-gas shift reaction at intermediate stages. The final product is not a water-gas shift reaction catalyst, and observation of the end of CO_2 production was used to monitor the completion of cluster formation.

Structure of Complex 1b. X-ray analysis establishes that crystals of **1b** contain two $[BPh_4]^-$ anions and one acetone molecule for each $[Pt_3(\mu\text{-}CO)(\mu\text{-}dmpm)_4]^{2+}$ cation. The shortest contacts between the different ions and molecules are in accord with the appropriate van der Waals radii. The acetone molecule and the $[BPh_4]^-$ anions show no unusual structural features (see Table I) and will not be considered further here.

(1) (a) University of Western Ontario. (b) University of Glasgow.
(2) Albinati, A. *Inorg. Chim. Acta* **1977**, *22*, L31. Moody, D. C.; Ryan, R. R. *Inorg. Chem.* **1977**, *16*, 1052.
(3) Bellon, P. L.; Ceriotti, A.; Demartin, F.; Longoni, G.; Heaton, B. T. *J. Chem. Soc., Dalton Trans.* **1982**, 1671.
(4) Ferguson, G.; Lloyd, B. R.; Puddephatt, R. J. *Organometallics* **1986**, *5*, 344.
(5) Albinati, A.; Carturan, G.; Musco, A. *Inorg. Chim. Acta* **1976**, *16*, L3.
(6) Hallam, M. F.; Howells, N. D.; Mingos, D. M. P.; Wardle, R. W. M. *J. Chem. Soc., Dalton Trans.* **1985**, 845.
(7) Moor, A.; Pregosin, P. S.; Venanzi, L. G. *Inorg. Chim. Acta* **1982**, *16*, L3.
(8) Browning, C. S.; Farrar, D. H.; Gukathasan, R. R.; Morris, S. A. *Organometallics* **1985**, *4*, 1750.
(9) Chatt, J.; Chini, P. *J. Chem. Soc. A* **1970**, 1538.
(10) Taylor, N. J.; Chieh, P. C.; Carty, A. J. *J. Chem. Soc., Chem. Commun.* **1975**, 448. Bender, R.; Braunstein, P.; Tiripicchio, A.; Camellini, M. T. *Angew. Chem., Int. Ed. Engl.* **1985**, *24*, 861.
(11) Bushnell, G. W.; Dixon, K. R.; Moroney, P. M.; Rattray, A. D.; Wan, C. *J. Chem. Soc., Chem. Commun.* **1977**, 709.
(12) Ferguson, G., personal communication. The bonding Pd–Pd distance is 2.579 (1) Å, and the two equivalent nonbonding Pd–Pd distances are 3.508 (1) Å.
(13) Bushnell, G. W.; Dixon, K. R.; Ono, R.; Pidcock, A. *Can. J. Chem.* **1984**, *62*, 696. Werner, H.; Bertlett, W.; Schubert, U. *Inorg. Chim. Acta* **1980**, *43*, 199.
(14) Underwood, D. J.; Hoffmann, R.; Tatsumi, K.; Nakamura, A.; Yamamoto, Y. *J. Am. Chem. Soc.* **1985**, *107*, 5968.
(15) Mingos, D. M. P.; Wardle, R. W. M. *Transition Met. Chem. (N.Y.)* **1985**, *10*, 441 and references therein.

0020-1669/87/1326-0231$01.50/0

Table I. Selected Distances (Å) and Angles (deg) for $[Pt_3(\mu\text{-CO})(\mu\text{-dmpm})_4][BPh_4]_2\cdot(CH_3)_2CO$

Bond Lengths

Pt(1)–Pt(2)	2.628 (1)	Pt(1)–Pt(3)	2.648 (1)	P(5)–C(51)	1.753 (23)	P(5)–C(52)	1.798 (27)
Pt(1)–P(1)	2.289 (3)	Pt(1)–P(6)	2.342 (3)	P(6)–C(3)	1.843 (14)	P(6)–C(61)	1.800 (15)
Pt(1)–P(8)	2.355 (3)	Pt(1)–C(5)	2.049 (8)	P(6)–C(62)	1.808 (13)	P(7)–C(4)	1.826 (11)
Pt(2)–Pt(3)	2.620 (1)	Pt(2)–P(2)	2.246 (3)	P(7)–C(71)	1.855 (15)	P(7)–C(72)	1.810 (20)
Pt(2)–P(3)	2.256 (3)	Pt(3)–P(4)	2.291 (3)	P(8)–C(4)	1.835 (12)	P(8)–C(81)	1.832 (13)
Pt(3)–P(5)	2.319 (3)	Pt(3)–P(7)	2.372 (3)	P(8)–C(82)	1.823 (14)	O–C(5)	1.194 (10)
Pt(3)–C(5)	2.061 (9)	P(1)–C(1)	1.823 (10)	O(s)–C(S1)	1.25 (3)	C(A1)–B(1)	1.697 (11)
P(1)–C(11)	1.824 (13)	P(1)–C(12)	1.810 (13)	C(B1)–B(1)	1.699 (12)	C(C1)–B(1)	1.700 (12)
P(2)–C(1)	1.832 (10)	P(2)–C(21)	1.808 (12)	C(D1)–B(1)	1.722 (12)	C(E1)–B(2)	1.683 (12)
P(2)–C(22)	1.809 (13)	P(3)–C(2)	1.816 (10)	C(F1)–B(2)	1.692 (11)	C(G1)–B(2)	1.710 (12)
P(3)–C(31)	1.812 (13)	P(3)–C(32)	1.801 (13)	C(H1)–B(2)	1.677 (12)	C(S1)–C(S2)	1.51 (3)
P(4)–C(2)	1.830 (10)	P(4)–C(41)	1.827 (12)	C(S1)–C(S3)	1.51 (3)		
P(4)–C(42)	1.812 (12)	P(5)–C(3)	1.833 (13)				

Bond Angles

Pt(2)–Pt(1)–Pt(3)	59.6 (1)	Pt(2)–Pt(1)–P(1)	91.2 (1)	Pt(2)–Pt(3)–P(4)	92.7 (1)	Pt(2)–Pt(3)–P(5)	151.3 (1)
Pt(2)–Pt(1)–P(6)	150.8 (1)	Pt(2)–Pt(1)–P(8)	94.8 (1)	Pt(2)–Pt(3)–P(7)	91.6 (1)	Pt(2)–Pt(3)–C(5)	61.0 (3)
Pt(2)–Pt(1)–C(5)	61.0 (3)	Pt(3)–Pt(1)–P(1)	146.0 (1)	P(4)–Pt(3)–P(5)	105.1 (1)	P(4)–Pt(3)–P(7)	103.9 (1)
Pt(3)–Pt(1)–P(6)	96.2 (1)	Pt(3)–Pt(1)–P(8)	95.1 (1)	P(4)–Pt(3)–C(5)	103.1 (3)	P(5)–Pt(3)–P(7)	105.3 (2)
Pt(3)–Pt(1)–C(5)	50.1 (3)	P(1)–Pt(1)–P(6)	104.9 (1)	P(5)–Pt(3)–C(5)	92.7 (3)	P(7)–Pt(3)–C(5)	142.1 (3)
P(1)–Pt(1)–P(8)	104.9 (1)	P(1)–Pt(1)–C(5)	102.3 (3)	P(1)–C(1)–P(2)	111.9 (5)	P(3)–C(2)–P(4)	112.5 (5)
P(6)–Pt(1)–P(8)	104.1 (1)	P(6)–Pt(1)–C(5)	91.4 (3)	P(5)–C(3)–P(6)	115.7 (8)	P(7)–C(4)–P(8)	113.6 (6)
P(8)–Pt(1)–C(5)	143.7 (3)	Pt(1)–Pt(2)–Pt(3)	60.6 (1)	Pt(1)–C(5)–Pt(3)	80.2 (3)	Pt(1)–C(5)–O	140.3 (7)
Pt(1)–Pt(2)–P(2)	97.8 (1)	Pt(1)–Pt(2)–P(3)	156.2 (1)	Pt(3)–C(5)–O	138.6 (7)	O(S)–C(S1)–C(S2)	113.3 (23)
Pt(3)–Pt(2)–P(2)	158.0 (1)	Pt(3)–Pt(2)–P(3)	97.0 (1)	O(S)–C(S1)–C(S3)	121.9 (23)	C(S2)–C(S1)–C(S3)	124.5 (23)
P(2)–Pt(2)–P(3)	103.7 (1)	Pt(1)–Pt(3)–Pt(2)	59.8 (1)	Pt–P–CH_2	107.9 (5)–111.7 (3)	B–C–C	118.0 (4)–121.9 (4)
Pt(1)–Pt(3)–P(4)	147.3 (1)	Pt(1)–Pt(3)–P(5)	95.2 (1)	Pt–P–CH_3	112.9 (4)–122.7 (5)	C–B–C	107.5 (7)–111.7 (7)
Pt(1)–Pt(3)–P(7)	94.9 (1)	Pt(1)–Pt(3)–C(5)	49.7 (3)	C–P–C	97.4 (10)–109.2 (9)		

Deviations of Atoms (Å) from Plane Defined by Pt(1), Pt(2), and Pt(3)

P(1)	0.716 (3)	P(2)	0.170 (3)	C(1)	0.034 (9)
P(4)	0.736 (3)	P(3)	0.333 (3)	C(2)	0.138 (9)
P(5)	0.592 (4)	P(6)	0.697 (3)	C(3)	0.268 (13)
P(7)	−2.363 (3)	P(8)	−2.343 (3)	C(5)	1.525 (8)

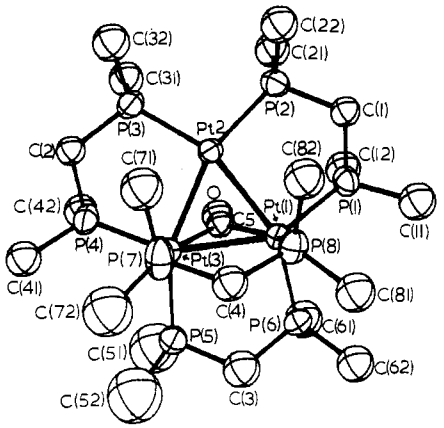

Figure 1. View of the $[Pt_3(\mu\text{-CO})(dmpm)_4]^{2+}$ cation showing 50% probability ellipsoids. Hydrogen atoms are omitted for clarity.

The novel 46e cluster cation shown in Figure 1 merits more detailed discussion. The skeleton of the cation is based on an isosceles triangle of platinum atoms edge bridged by three latitudinal dmpm ligands. The Pt(1)–Pt(3) bond is further supported by longitudinally bridging carbonyl and dmpm ligands; thus the Pt(1)Pt(3)C(5)O and Pt(1)Pt(3)P(7)P(8) planes are approximately normal to the Pt_3 triangle (respective dihedral angles are 102 and 91°). The point symmetry of the cation is therefore close to C_s: the noncrystallographic symmetry plane is normal to the Pt_3 triangle and passes through the atoms Pt(2), C(3), C(4), C(5), and O.

The geometry of the latitudinal $Pt_3(dmpm)_3$ core of the cation reflects the presence of the longitudinal dmpm ligand in two ways. First, the Pt–P bonds involving the atoms P(1) to P(6) are bent out of the Pt_3 plane and away from P(7) and P(8), the out-of-plane displacements (Table I) being greater for the phosphorus atoms attached to Pt(1) and Pt(3) than for those attached to Pt(2). Second, the three latitudinal Pt_2P_2C rings adopt envelope conformations, with P–Pt–Pt–P torsion angles close to 0°; in consequence, their *P*-methyl substituents can be regarded as either pseudoaxial, with the P–C bond roughly normal to the Pt_3 plane, or pseudoequatorial, with the P–C bond roughly parallel with the Pt_3 plane. The methylene carbon atoms C(1), C(2), and C(3) are each displaced from the Pt_3 plane less than the phosphorus atoms to which they are bonded. In consequence, only pseudoequatorial methyl carbon atoms (C(11), C(22), C(32), C(41), C(52), and C(62)) can protrude above the Pt_3 plane toward the P(7),P(8) dmpm ligand. The out-of-plane bending of the Pt–P bonds and the absence of pseudoaxial methyl groups pointing toward the P(7),P(8) dmpm ligand help to relieve interligand contacts within the cation. The most significant of these contacts involve C(21)···C(31), C(71)···C(2), C(72)···C(52), C(81)···C(62), and C(82)···C(1) separations of 3.73–3.85 Å, which are only slightly shorter than the van der Waals diameter of a methyl carbon atom (4.0 Å).

Whatever view may be taken of the bonding in the cation (see Discussion) it is clear that the Pt(2) center differs both electronically and sterically from Pt(1) and Pt(3). This difference has little effect on the Pt–Pt bond lengths: the Pt(1)–Pt(3) distance (2.648 (1) Å) is only marginally longer than the effectively equal Pt(1)–Pt(2) and Pt(2)–Pt(3) distances (2.628 (1) and 2.620 (1) Å). More remarkably, the mean Pt–Pt bond length of 2.632 Å in **1b**, a 46e species, is virtually the same as the corresponding average values of 2.634 and 2.623 Å for the related 42e and 44e species $[Pt_3(\mu_3\text{-CO})(dppm)_3]^{2+}$ and $[Pt_3(SCN)(\mu_3\text{-CO})(dppm)_3]^{+}$.[4,16] This would seem to imply that the extra electrons in **1** do not occupy strongly antibonding cluster orbitals.

In comparison with the case for the Pt–Pt distances, the Pt–P bond lengths show greater sensitivity to environment. The shortest Pt–P bonds (mean length 2.25 Å) involve the four-coordinate Pt(2) atom. Next in length are the latitudinal Pt–P bonds from Pt(1) and Pt(3): the Pt(1)–P(1) and Pt(3)–P(4) distances (mean 2.29 Å) are slightly shorter than the Pt(1)–P(6) and Pt(3)–P(5) bond lengths (mean 2.33 Å); similar values of 2.26–2.31 Å are found

(16) Ferguson, G.; Lloyd, B. R.; Manojlović-Muir, Lj.; Muir, K. W.; Puddephatt, R. J. *Inorg. Chem.* **1986**, *25*, 4190.

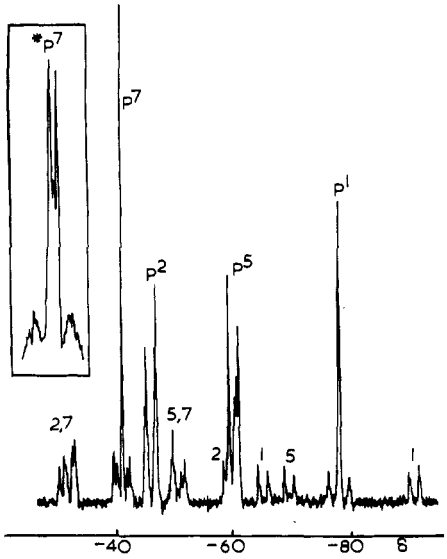

Figure 2. $^{31}P\{^1H\}$ NMR spectrum of complex **1a**, with tentative assignments (atom numbers defined in Figure 1). The satellites due to $^1J(PtP)$ couplings are indicated, and the inset shows the resonance due to P(7),P(8) in the ^{13}C-labeled complex, **1a***.

for comparable distances in related 42e and 44e complexes based on the $[Pt_3(CO)(dppm)_3]$ framework.[4,16] The longest Pt–P bonds in **1b** involve P(7) and P(8); their mean length of 2.36 Å is comparable with that of 2.376 (7) Å for the single latitudinal Pt–P bond in the severely overcrowded 44e species $[Pt_3(\mu\text{-}SO_2)_3\{P(C_6H_{11})_3\}_2\{Ph_2P(CH_2)_3PPh_2\}]$.[6]

Other dimensions in the cation are normal. The μ-CO bridge is symmetrical. The mean P–CH_2 and P–CH_3 distances are 1.830 (3) and 1.811 (5) Å. The P···P bite distances (3.028 (4)–3.113 (4) Å) are typical of diphosphinomethane bridging groups and and consistent with P–C–P angles (112–116°) only slightly greater than the tetrahedral value.

Characterization by Spectroscopic Methods. When the structure of **1b** was known, the spectroscopic data could be interpreted. The IR spectrum of **1** contained a band at 1730 cm^{-1} due to the bridging carbonyl group. The ^1H NMR spectrum gave complex resonances due to the *Me*P and CH_2P_2 groups and gave no useful structural information. However, integration of the ^1H NMR spectrum showed that **1b** contained two $[BPh_4]^-$ ions per cluster unit, thus showing that the cluster carried a 2+ charge; this was also indicated by the analytical data.

The ^{195}Pt NMR spectrum of **1** contained two resonances, a broad triplet with $^1J(PtP) \approx 3000$ Hz due to Pt(2)[17] and a doublet of doublets with $^1J(PtP) = 3060$, 2500, and 2250 Hz due to Pt(1) and Pt(3). Approximately the same coupling constants were observed in the ^{31}P NMR spectrum, as described below.

The ^{31}P NMR spectrum of **1** contained four resonances of approximately equal intensity (Figure 2), two of which appeared as singlets with ^{195}Pt satellites and two as doublets with a large $J(PP)$ coupling of 210 Hz. The ^{195}Pt satellites of the singlet resonances also appeared as doublets with $J(PP) = 210$ Hz. The chemically equivalent pairs of ^{31}P atoms are as follows: P(1),P(4); P(2),P(3); P(5),P(6); P(7),P(8). For a singlet resonance with doublet ^{195}Pt satellites, the coupling $J(PP)$ of 210 Hz must be between chemically equivalent ^{31}P atoms bound to different platinum atoms. This is the case for all pairs except for P(2),P(3); therefore, these phosphorus atoms must appear as a doublet in the ^{31}P NMR spectrum, and the signal at $\delta = -46$ with $^1J(Pt^2P^2) = 3135$ Hz is assigned since this coupling constant is consistent with that observed in the ^{195}Pt NMR spectrum for Pt(2).[17] The large $J(PP)$ coupling is expected to be $^3J(P^2P^5)$ and $^3J(P^3P^6)$, a trans-like coupling through a Pt–Pt bond.[4] Hence, the second doublet signal is assigned as due to P(5) and P(6), with $^1J(PtP) = 2250$ Hz. The assignment of the singlet signals (Figure 2) is based on the correlation of $^1J(PtP)$ with the Pt–P bond distance.[18] Thus the signal at $\delta = -78$ with $^1J(PtP) = 3060$ Hz is assigned to P(1),P(4) and the signal at $\delta = -42$ with $^1J(PtP) = 2500$ Hz is assigned to P(7),P(8), since the respective Pt–P distances are 2.29 and 2.36 Å, respectively. In the ^{31}P NMR spectrum of **1*** (asterisk indicates ^{13}CO-labeled complex, see below), the signal due to P(7),P(8) was split into a doublet with $J(PC) = 57.5$ Hz, but no other PC couplings were observed. This observation is reasonable since the ^{13}CO and the dmpm ligand defined by P(7),P(8) are mutually trans, whereas the other dmpm ligands are approximately orthogonal to the carbonyl ligand.

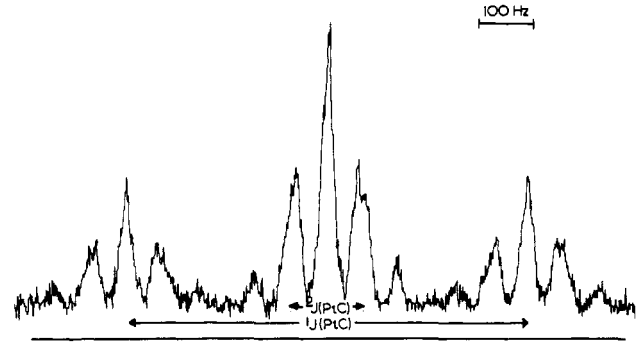

Figure 3. ^{13}C NMR spectrum (75.6 MHz) of complex **1a***, showing only the carbonyl resonance. The central triplet is due to $^2J(PC)$ coupling, and the centers of the major satellites due to coupling to ^{195}Pt are indicated below. Only the inner three lines of the 1:8:18:8:1 quintet due to $^1J(PtC)$ coupling are shown; the outer lines were barely resolved.

In the ^{13}C NMR spectrum of **1***, the carbonyl resonance appeared as a triplet due to coupling to P(7),P(8) with $J(PC) = 57$ Hz, with complex satellites due to coupling to ^{195}Pt (Figure 3). The coupling $^1J(PtC) = 730$ Hz and the expected 1:8:18:8:1 multiplet[19] for a doubly bridging group was observed. In addition, the long-range coupling $^2J(Pt^2C) = 130$ Hz gave rise to one-fourth-intensity satellites, which overlapped with the central triplet, giving a distorted-quintet appearance (Figure 3). These data show clearly that the solid-state structure is maintained in solution.

Reactivity of the $[Pt_3(\mu\text{-}CO)(\mu\text{-}dmpm)_4]^{2+}$ Ion. In view of the theory that the 42e configuration is favored for Pt_3 clusters,[14] it was considered possible that one of the dmpm ligands or the CO ligand of **1** might be displaced readily. The cation **1** has one 16e platinum center, and so an associative mechanism (as well as a dissociative mechanism) for such a displacement is possible. However, the cation **1** was found to be very robust and no reaction occurred with the reagents CS_2, SO_2, H_2S, HCCH, PhCCPh, $MeO_2CC{\equiv}CCO_2Me$, or $NaBH_4$ as monitored by ^{31}P NMR spectroscopy. For example $[1][PF_6]_2$ could be dissolved in liquid SO_2 and allowed to stand for several days in the dark or exposed to UV radiation but no reaction occurred (the reaction was monitored in situ by ^{31}P NMR spectroscopy) and the starting material was recovered. In contrast, sulfur dioxide easily displaces CO from the 42e clusters $[Pt_3(\mu\text{-}CO)_3(PR_3)_3]$,[15] and all of the above reagents react readily with the 42e cluster[4,20] $[Pt_3(\mu_3\text{-}CO)(\mu\text{-}dppm)_3]^{2+}$. Successful reactions were observed between **1** and ^{13}CO, MeNC, and I_2. Excess ^{13}CO reacts slowly with **1** over a period of ~1 day to give **1*** by displacement of ^{12}CO with ^{13}CO. Complex **1*** was characterized by its NMR spectrum, as discussed above. The reaction is much slower than the exchange of ^{13}CO for ^{12}CO in $[Pt_3(\mu_3\text{-}CO)(\mu\text{-}dppm)_3]^{2+}$, which occurs rapidly on the NMR time scale at room temperature.[20] Similarly, methyl isocyanide displaced CO from **1** to give $[Pt_3(\mu\text{-}CNMe)(\mu\text{-}dmpm)_4]^{2+}$, characterized by elemental analysis, by

(17) This peak in the ^{195}Pt NMR spectrum was broad, and $^1J(PtP)$ is estimated as 3000 ± 200 Hz. The accurate coupling constant obtained from the ^{31}P NMR spectrum was 3135 cm^{-1}.

(18) Pidcock, A. *Catalytic Aspects of Metal Phosphine Complexes*; Alyea, E. C., Meek, D. W., Eds.; Advances in Chemistry 196; American Chemical Society: Washington, DC, 1982; p 1.
(19) Goggin, P. L.; Goodfellow, R. J.; Reed, F. J. S. *J. Chem. Soc. A* **1971**, 2031.
(20) Lloyd, B. R.; Puddephatt, R. J., unpublished work.

Table II. Fractional Coordinates and Displacement Parameters (Å^2) for $[Pt_3(\mu\text{-CO})(\mu\text{-dmpm})_4][BPh_4]_2\cdot(CH_3)_2CO$

	x/a	y/b	z/c	U[a]		x/a	y/b	z/c	U[a]
Pt(1)	−0.20355 (1)	0.28407 (2)	−0.00131 (1)	0.038	C(B5)	0.8583 (3)	−0.0652 (5)	0.3357 (2)	0.073 (3)
Pt(2)	−0.19199 (1)	0.14721 (2)	0.07375 (1)	0.038	C(B6)	0.8408 (4)	0.0163 (4)	0.3575 (5)	0.062 (2)
Pt(3)	−0.29738 (1)	0.18263 (1)	0.00611 (1)	0.042	C(C1)	0.8974 (5)	0.2029 (9)	0.4538 (3)	0.060 (2)
P(1)	−0.11489 (10)	0.34809 (17)	0.04791 (11)	0.052	C(C2)	0.9057 (3)	0.2872 (7)	0.4824 (5)	0.072 (3)
P(2)	−0.09517 (10)	0.16957 (17)	0.11748 (10)	0.049	C(C3)	0.9393 (5)	0.2916 (5)	0.5387 (4)	0.076 (3)
P(3)	−0.22278 (11)	0.04266 (17)	0.13107 (10)	0.049	C(C4)	0.9647 (4)	0.2118 (7)	0.5664 (3)	0.082 (3)
P(4)	−0.34618 (11)	0.10355 (17)	0.06454 (11)	0.054	C(C5)	0.9564 (4)	0.1276 (6)	0.5378 (5)	0.079 (3)
P(5)	−0.36770 (12)	0.28535 (26)	−0.04612 (17)	0.087	C(C6)	0.9228 (6)	0.1231 (6)	0.4814 (4)	0.070 (3)
P(6)	−0.25804 (11)	0.40869 (18)	−0.05138 (11)	0.056	C(D1)	0.8637 (3)	0.2897 (5)	0.3439 (3)	0.056 (2)
P(7)	−0.28337 (14)	0.06912 (22)	−0.06173 (12)	0.072	C(D2)	0.9179 (4)	0.3355 (9)	0.3555 (4)	0.070 (3)
P(8)	−0.17892 (11)	0.19283 (17)	−0.07434 (10)	0.053	C(D3)	0.9274 (4)	0.4067 (8)	0.3198 (3)	0.081 (3)
O	−0.2597 (3)	0.3321 (5)	0.0993 (3)	0.063 (2)	C(D4)	0.8827 (3)	0.4320 (4)	0.2725 (3)	0.084 (3)
O(S)	0.4961 (8)	0.1914 (14)	0.3358 (8)	0.206 (7)	C(D5)	0.8284 (4)	0.3861 (8)	0.2609 (4)	0.075 (3)
C(1)	−0.0612 (4)	0.2587 (7)	0.0805 (4)	0.052 (2)	C(D6)	0.8190 (4)	0.3149 (7)	0.2966 (3)	0.066 (3)
C(2)	−0.2999 (4)	0.0079 (6)	0.1015 (4)	0.050 (2)	C(E1)	0.6113 (4)	0.2635 (9)	0.5879 (3)	0.061 (2)
C(3)	−0.3327 (6)	0.3650 (9)	−0.0883 (6)	0.084 (3)	C(E2)	0.5994 (4)	0.1890 (6)	0.5502 (5)	0.079 (3)
C(4)	−0.2418 (5)	0.1191 (7)	−0.1107 (5)	0.065 (3)	C(E3)	0.5667 (5)	0.2021 (5)	0.4941 (4)	0.080 (3)
C(5)	−0.2533 (4)	−0.2865 (6)	0.0593 (4)	0.043 (2)	C(E4)	0.5458 (4)	0.2897 (7)	0.4757 (3)	0.078 (3)
C(11)	−0.0720 (6)	0.4174 (9)	0.0079 (6)	0.084 (3)	C(E5)	0.5577 (4)	0.3641 (5)	0.5133 (5)	0.075 (3)
C(12)	−0.1192 (6)	0.4238 (9)	0.1075 (5)	0.082 (3)	C(E6)	0.5904 (6)	0.3510 (7)	0.5694 (4)	0.064 (2)
C(21)	−0.0812 (5)	0.2117 (8)	0.1910 (5)	0.076 (3)	C(F1)	0.7280 (3)	0.2483 (8)	0.6538 (4)	0.051 (2)
C(22)	−0.0433 (5)	0.0735 (8)	0.1229 (5)	0.076 (3)	C(F2)	0.7455 (4)	0.2302 (9)	0.6034 (3)	0.060 (2)
C(31)	−0.2223 (5)	0.0887 (9)	0.2020 (5)	0.077 (3)	C(F3)	0.8054 (4)	0.2244 (5)	0.6043 (3)	0.066 (3)
C(32)	−0.1840 (6)	−0.0662 (9)	0.1492 (5)	0.079 (3)	C(F4)	0.8480 (2)	0.2366 (6)	0.6555 (4)	0.066 (3)
C(41)	−0.4177 (5)	0.0480 (8)	0.0319 (5)	0.075 (3)	C(F5)	0.8305 (4)	0.2546 (8)	0.7059 (2)	0.068 (3)
C(42)	−0.3654 (5)	0.1685 (8)	0.1227 (5)	0.072 (3)	C(F6)	0.7705 (4)	0.2605 (4)	0.7051 (4)	0.063 (2)
C(51)	−0.4101 (11)	0.3498 (16)	−0.0079 (11)	0.168 (8)	C(G1)	0.6389 (4)	0.1418 (5)	0.6799 (4)	0.064 (2)
C(52)	−0.4257 (12)	0.2424 (19)	−0.1050 (11)	0.183 (9)	C(G2)	0.6824 (5)	0.0876 (10)	0.7150 (5)	0.063 (2)
C(61)	−0.2687 (6)	0.5038 (10)	−0.0057 (6)	0.095 (4)	C(G3)	0.6672 (4)	0.0041 (10)	0.7362 (6)	0.073 (3)
C(62)	−0.2373 (6)	0.4661 (9)	−0.1112 (5)	0.081 (3)	C(G4)	0.6084 (4)	−0.0253 (5)	0.7223 (4)	0.117 (5)
C(71)	−0.2392 (6)	0.0360 (10)	−0.0334 (6)	0.092 (4)	C(G5)	0.5649 (4)	0.0289 (10)	0.6872 (5)	0.194 (10)
C(72)	−0.3461 (8)	0.0179 (13)	−0.1131 (8)	0.128 (6)	C(G6)	0.5802 (4)	0.1124 (10)	0.6660 (7)	0.127 (6)
C(81)	−0.1592 (5)	0.2486 (9)	−0.1364 (5)	0.080 (3)	C(H1)	0.6414 (7)	0.3321 (5)	0.6989 (6)	0.060 (2)
C(82)	−0.1178 (6)	0.1096 (9)	−0.0537 (5)	0.084 (3)	C(H2)	0.6000 (5)	0.3188 (6)	0.7315 (4)	0.083 (3)
C(A1)[b]	0.7800 (3)	0.1941 (8)	0.3880 (4)	0.057 (2)	C(H3)	0.5858 (3)	0.3910 (5)	0.7640 (4)	0.097 (4)
C(A2)	0.7622 (4)	0.2291 (9)	0.4352 (2)	0.059 (2)	C(H4)	0.6131 (5)	0.4765 (5)	0.7639 (5)	0.090 (4)
C(A3)	0.7025 (4)	0.2281 (5)	0.4360 (4)	0.061 (2)	C(H5)	0.6545 (4)	0.4899 (6)	0.7314 (3)	0.092 (4)
C(A4)	0.6607 (2)	0.1921 (6)	0.3896 (4)	0.072 (3)	C(H6)	0.6686 (4)	0.4177 (5)	0.6989 (5)	0.068 (3)
C(A5)	0.6784 (4)	0.1571 (8)	0.3425 (2)	0.081 (3)	C(S1)	0.5057 (10)	0.2313 (16)	0.2926 (10)	0.142 (7)
C(A6)	0.7381 (5)	0.1581 (4)	0.3417 (4)	0.069 (3)	C(S2)	0.4985 (11)	0.3357 (18)	0.2940 (11)	0.174 (9)
C(B1)	0.8718 (5)	0.0977 (3)	0.3549 (5)	0.052 (2)	C(S3)	0.5171 (11)	0.1775 (17)	0.2416 (10)	0.163 (8)
C(B2)	0.9204 (4)	0.0976 (5)	0.3304 (3)	0.057 (2)	B(1)	0.8530 (5)	0.1963 (8)	0.3856 (5)	0.056 (3)
C(B3)	0.9379 (3)	0.0161 (4)	0.3086 (4)	0.069 (3)	B(2)	0.6548 (5)	0.2480 (8)	0.6549 (5)	0.055 (2)
C(B4)	0.9069 (4)	−0.0653 (3)	0.3112 (4)	0.077 (3)					

[a] U is the mean latent root of the U_{ij} tensor for Pt and P atoms. Otherwise it is the refined isotropic displacement parameter. [b] Phenyls A–H were refined as rigid groups.

an IR band at 1706 cm^{-1} due to ν(N≡C), and by the ^{1}H and ^{31}P NMR spectra (Experimental Section), which were very similar to those for **1**. The reaction with iodine was rapid and led to breakdown of the cluster with formation of $[PtI_2(dmpm)]$. The stability of the cluster is illustrated by the reaction with cyanide, which gave an insoluble complex, characterized as $[\mathbf{1}](CN)_2$. The IR spectrum contained bands at 2131 and 2120 cm^{-1}, in the region for ionic cyanide, and the UV–visible spectrum contained bands at 253 and 357 nm, in essentially the same positions as for $[\mathbf{1}][PF_6]_2$ (254 and 356 nm) in solution. The complex was too insoluble for NMR spectroscopy.

Together these reactions indicate that the cation **1** may be considered to be coordinatively saturated, since there is no tendency to add an extra ligand to the 16e center Pt(2), and the displacement of CO by ^{13}CO or MeNC is slow. However, there is no evidence that the 46e cation **1** is unstable and the dmpm ligands are certainly not labile.

Discussion

It is interesting that dmpm forms the 46e cluster cation $[Pt_3(\mu\text{-CO})(\mu\text{-dmpm})_4]^{2+}$ whereas dppm forms[4] the 42e cluster $[Pt_3(\mu_3\text{-CO})(\mu\text{-dppm})_3]^{2+}$. The difference is presumably due to the lower steric bulk of dmpm.[21] Curiously, the addition of the extra chelate ligand causes the carbonyl to move to a μ position, *toward* the platinum centers with higher coordination number (eq 2).

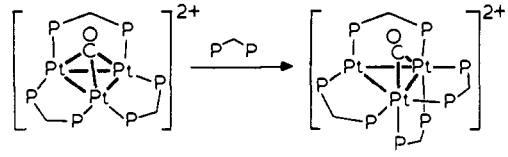

(2)

This may indicate that the carbonyl acts primarily as an electron acceptor and binds to the centers of maximum electron density in complex **1**. We note that the presence of a μ-carbonyl in **1** facilitates electron counting. Thus, if it is accepted that each platinum forms two metal–metal bonds and if the positive charges are placed on Pt(1) and Pt(3), then Pt(1) and Pt(3) have 18e counts while Pt(2) has a 16e count.

The high electron counts for Pt(1) and Pt(3) do not appear to lead to any weakening of Pt–Pt interactions of the kind observed in all other cases,[2-7,10-15] even though the Pt–P bonds at these centers are somewhat longer than those at Pt(2). Previous cases involving low-oxidation-state complexes, such as the 42e $[Pt_3(CO)_3L_3]$ and 44e $[Pt_3(CO)_3L_4]$, have involved bulky ligands L, and the modest increases in Pt–Pt bond distances for the 44e complexes may be due primarily to steric effects.[2,5,6] The rule that increasing the electron count above 42e leads to lengthening of metal–metal bonds for trinuclear complexes of platinum and palladium[14] ap-

(21) Ling, S. S. M.; Jobe, I. R.; McLennan, A. J.; Manojlović-Muir, Lj.; Muir, K. W.; Puddephatt, R. J. *J. Chem. Soc., Chem. Commun.* **1985**, 566.

pears most useful in higher oxidation state complexes, where there is a greater tendency for the metals to use only eight orbitals in bonding, and clearly does not apply to the cation **1**. Here it seems that two of the platinum atoms use all nine valence orbitals in bonding.

The ability of these clusters to add additional ligands without breaking apart suggests an interesting chemistry, which could model chemisorption and catalysis at a platinum surface. Further studies in this area are in progress.

Experimental Section

NMR spectra were recorded with Varian XL100 or XL200 spectrometers. The complex $[Pt_2(\mu\text{-dmpm})_3(PPh_3)]$ was prepared as described previously.[21]

$[Pt_3(\mu\text{-CO})(\mu\text{-dmpm})_4][PF_6]_2$. The complex $[Pt_2(\mu\text{-dmpm})_3(PPh_3)]$ (0.21 g) in a sealed glass tube was placed in a Parr pressure reactor (300-mL capacity) containing CH_3OH/H_2O (75 mL, 2:1 mixture). The reactor was purged with CO and then charged to 60 psi with CO and heated to 100 °C. The stirrer was turned on to crush the glass tube, and the mixture was allowed to react for 6 h, by which time production of CO_2 (0.4 mmol) and hydrogen had ceased. The mixture was cooled, the reactor was opened, and the methanol was evaporated to leave an orange aqueous solution. To this solution was added $NH_4[PF_6]$ (0.65 g) in MeOH (6 mL), and the orange precipitate of the product was separated by filtration, washed with water and methanol, and dried under vacuum; yield 0.134 g. It was recrystallized from acetone/hexane as orange–red needles. Anal. Calcd for $[Pt_3(CO)(dmpm)_4][PF_6]_2\cdot(CH_3)_2CO$: C, 19.1; H, 4.1. Found: C, 18.5; H, 4.3.

The complex $[Pt_3(CO)(dmpm)_4][BPh_4]_2$ was prepared similarly by reaction of the aqueous solution of the cation with $Na[BPh_4]$. Anal. Calcd for $[Pt_3(CO)(dmpm)_4][BPh_4]_2$: C, 46.1; H, 5.3. Found: C, 46.1; H, 5.6. NMR (acetone-d_6): ^1H, δ 1.50–1.89 [m, CH_3P], 2.84–5.72 [m, CH_2P_2]; ^{31}P, δ −41.9 [s, $^1J(PtP) = 2592$, $^2J(PtP) = 110$, $^3J(PP) = 210$, P^7, P^8], −46.5 [d, $^1J(PtP) = 3328$, $^3J(PP) = 210$, P^2, P^3], −60.2 [d, $^1J(PtP) = 2285$, $^3J(PP) = 210$, P^1, P^4], −78.0 [s, $^1J(PtP) = 3072$, $^2J(PtP) = 192$, $^3J(PP) = 210$, P^5, P^6].

Crystal Structure of $[Pt_3(\mu\text{-CO})(\mu\text{-dmpm})_4][BPh_4]_2\cdot(CH_3)_2CO$. The specimen was a dark red plate of dimensions 0.65 × 0.30 × 0.15 mm grown from toluene/acetone solution. All measurements were made with Mo Kα X-rays, λ = 0.710 69 Å, on an Enraf-Nonius CAD4F diffractometer equipped with a graphite monochromator.

Crystal data: $C_{72}H_{102}B_2O_2P_8Pt_3$, M_r = 1854.3, monoclinic, space group $P2_1/n$, a = 23.040 (2) Å, b = 14.367 (1) Å, c = 23.823 (1) Å, β = 103.95 (1)°, U = 7653 Å^3, Z = 4, D_{calcd} = 1.609 g cm^{-3}, $F(000)$ = 3656, $\mu(\mu o\ K\alpha)$ = 57.3 cm^{-1}, T = 295 K.

Unit cell dimensions and crystal orientation were determined by a least-squares fit to the setting angles, averaged over four diffraction positions, of 23 reflections with $13 < \theta < 18°$.[22] The space group was determined from the systematic absences.

The intensities of 14 377 reflections with $2 \leq \theta(Mo\ K\alpha) \leq 25°$ were measured from $\theta/2\theta$ scans of $(0.64 + 0.35 \tan\theta)°$ in θ; background was estimated by extending the scan by 25% at each end. A fast initial scan was used to adjust the final scan speed so as to obtain $\sigma(I)/I \leq 0.02$, subject to a maximum counting time of 120 s. Correction was made for Lorentz–polarization and absorption effects, the latter by an empirical method,[23] which gave transmission factors on F of 0.83–1.29. Corrections for crystal decomposition and extinction were not deemed necessary. Merging 358 duplicate measurements (R_{int} = 0.026) gave 13 410 independent structure amplitudes, of which 8106 with $I \geq \sigma(I)$ were used in subsequent calculations.

The structure was solved by Patterson and difference Fourier methods and refined by full-matrix least squares, with $w = \exp(5.5(\sin^2\theta)/\lambda^2)/[\sigma^2(F) + 0.00023F^2]$. The eight phenyl rings were treated as rigid groups, with C–C = 1.380 Å and C–H = 0.96 Å. Methyl and methylene hydrogen positions were deduced from geometrical considerations (C–H = 0.96 Å) and were allowed to ride on the carbon atoms to which they are bonded, with $U(H) = U(C)$. Only the acetone hydrogen atoms were omitted from the final structure factor calculations. Anisotropic displacement parameters were used only for Pt and P atoms. Refinement of 308 structure parameters converged ($\Delta/\sigma < 0.20$) with R = 0.032, R_w = 0.042, and S = 1.95. Final $|\Delta\rho|$ values did not exceed 1.1 e Å^{-3}. Neutral-atom scattering factors and complex anomalous dispersion corrections were taken from ref 24. Calculations were performed with the GX package[25] on a Gould 3227 computer. Final atomic coordinates are listed in Table II.

Enrichment of $[Pt_3(\mu\text{-dmpm})_4(\mu\text{-CO})][PF_6]_2$ with ^{13}CO(g). $[Pt_3(\mu\text{-dmpm})_4(\mu\text{-CO})][PF_6]_2$ (0.03 g, 0.02 mmol) was dissolved in $(CD_3)_2CO$ (~1 mL) and filtered into a 5-mm NMR tube fitted with a Teflon tap. This tube was attached to a vacuum line along with a 100-mL vessel containing 99% ^{13}CO(g). The sample was degassed under vacuum and frozen to −100 °C. ^{13}CO was introduced to the sample and condensed in the tube. The tube was sealed and left to warm to room temperature, and the reaction was monitored by NMR spectroscopy.

Reaction of $[Pt_3(\mu\text{-dmpm})_3(CO)][PF_6]_2$ with MeNC. To a solution of $[Pt_3(\mu\text{-dmpm})_3(CO)][PF_6]_2$ (0.04 g, 0.03 mmol) in acetone (3 mL) was added methyl isocyanide (0.01 g, 0.3 mmol) dropwise. No immediate change was apparent, and the mixture was stirred for 1 h. Pentane was added to precipitate the product, which was isolated, washed with pentane (2 × 5 mL), and dried to yield an orange crystalline solid identified as $[Pt_3(\mu\text{-dmpm})_3(MeNC)][PF_6]_2$ (0.03 g, 0.02 mmol, 66%). Crystals of the product were obtained from an acetone/pentane mixture. Anal. Calcd for $C_{22}H_{59}NP_{10}F_{12}P_3$: C, 18.1; H, 4.0;, N, 1.0. Found: C, 18.4; H, 3.9; N, 1.4. IR: ν(MeN–C) 1706 cm^{-1}, ν(P–F) 840 cm^{-1}. ^1H NMR: δ 1.65 [br, m, PCH_3], 1.71 [br, m, PCH_3], 3.3 [br, s, NCH_3], 2.8–5.5 [complex, CH_2P_2]. ^{31}P NMR: δ −49.2 [s, $^1J(PtP) = 2760$, $^2J(PtP) = 70$ Hz], −52.4 [d, $^1J(PtP) = 2820$, $^2J(PP) = 200$ Hz], −63.2 [$^1J(PtP) = 2040$ Hz, $^2J(PP) = 200$ Hz], −82.5 [s, $^1J(PtP) = 2980$, $^2J(PtP) = 200$ Hz].

Reaction of $[Pt_3(\mu\text{-dmpm})_4(\mu\text{-CO})][PF_6]_2$ with KCN. To a solution of $[Pt_3(\mu\text{-dmpm})_4(\mu\text{-CO})][PF_6]_2$ (40 mg, 0.03 mmol) in acetone (2 mL) was added solid KCN (5 mg, 0.07 mmol), and the mixture was stirred for 24 h. This resulted in the formation of an orange precipitate. The solvent was decanted, and the precipitate was washed with water (5 mL) to remove excess KCN and then dried to yield the product (25 mg). The solid was insoluble in acetone, CH_2Cl_2, $CHCl_3$, and water and so could not be adequately purified. Anal. Calcd for $C_{23}H_{48}N_2OP_8Pt_3$: C, 22.8; H, 4.6; N, 2.3. Found: C, 20.4; H, 3.8; N, 2.6. IR: ν(CN) = 2131, 2120 cm^{-1}; ν(PF) absent.

Reaction of $[Pt_3(\mu\text{-dmpm})_3(\mu\text{-CO})][PF_6]_2$ with I_2. To a red solution of $[Pt_3(\mu\text{-dmpm})_3(\mu\text{-CO})][PF_6]_2$ (0.03 g, 0.21 mmol) in acetone (3 mL) that was being stirred was added in small portions iodine (0.01 g, 0.04 mmol) in acetone (5 mL). A reaction was evident from the color change of the mixture from dark red to light orange together with the formation of a considerable amount of a white precipitate of $[PtI_2(dmpm)]$. The precipitate was separated, washed with pentane, and dried. Anal. Calcd for $C_5H_{12}P_2I_2Pt$: C, 10.3; H, 2.4. Found: C, 9.8; H, 2.5. ^{31}P NMR: δ −84.4 [s, $^1J(PtP) = 2770$ Hz].

Acknowledgment. We are grateful for the financial support of Glasgow University and the SERC (Great Britain) (Lj.M.-M. and K.W.M.) and of the NSERC (Canada) (S.S.M.L. and R. J.P.).

Registry No. **1a**, 105931-27-9; **1b**·$(CH_3)_2CO$, 105931-29-1; $[Pt_2(\mu\text{-dmpm})_3(PPh_3)]$, 98965-01-6; $[Pt_3(\mu\text{-dmpm})_3(MeNC)][PF_6]_2$, 105931-31-5; $[PtI_2(dmpm)]$, 97336-91-9; $[Pt_3(\mu\text{-dmpm})_3(CO)][PF_6]_2$, 105943-55-3; KCN, 151-50-8; I_2, 7553-56-2.

Supplementary Material Available: Tables of anisotropic displacement parameters, calculated hydrogen atom positions, and bond angles (6 pages); a listing of observed and calculated structure factors (33 pages). Ordering information is given on any current masthead page.

(22) De Boer, J. L.; Duisenberg, A. J. M. "Enraf-Nonius CAD4F Diffractometer Software Update Feb-84"; Enraf-Nonius: Groningen and Utrecht, The Netherlands, 1984.
(23) Walker, N.; Stuart, D. *Acta Crystallogr., Sect. A: Found. Crystallogr.* **1983**, *A39*, 158.
(24) *International Tables for X-ray Crystallography*; Kynoch: Birmingham, England, 1974; Vol. IV, pp 99, 149.
(25) Mallinson, P. R.; Muir, K. W. *J. Appl. Crystallogr.* **1985**, *18*, 51.